Mixed Monolayers for the Design of Structured Surfaces To Induce Oriented 3-D Crystallization

I. Weissbuch,[*,†] **J. Majewski,**[†] **K. Kjaer,**[‡] **J. Als-Nielsen,**[‡] **M. Lahav,**[*,†] **and L. Leiserowitz**[*,†]

Department of Materials & Interfaces, The Weizmann Institute of Science, 76100 Rehovot, Israel, and Physics Department, Risø National Laboratory, DK4000 Roskilde, Denmark

Received: June 15, 1993[●]

Mixed monolayers containing two different amphiphiles $C_{19}H_{39}CONHCH_2CH_2CO_2H$ (**A**) and $C_{19}H_{39}CONH_2$ (**B**) were designed in order to form a two-dimensional (2-D) crystalline solid solution in which the **A**-type molecules form domains within the sea of **B**-type molecules. A "continuous" 2-D arrangement of the aliphatic chains was expected, driven by the amide hydrogen bonding requirement; a tendency for the formation of the embeded **A**-type domains should be provided by the interactions between the $-CH_2CH_2CO_2H$ head group moieties. The mixed monolayers served to promote the oriented nucleation of silver propionate 3-D crystals attached at the monolayer–solution interface. Only the **A**-type domains induced silver propionate crystallization whereas the **B**-type domains were essentially inert. The mixed **A** + **B** monolayers were found to be efficient nucleators down to a 1:10 molar ratio, providing proof for the existence of **A**-type domains. Additional information such as the structure and ion-binding properties of the mixed monolayers was furnished by specular X-ray reflectivity and grazing incidence X-ray diffraction using synchrotron radiation.

Introduction

Recent studies have shown that amphiphilic molecules, in the form of Langmuir monolayer films spread over supersaturated aqueous solutions, can induce the formation of oriented three-dimensional (3-D) crystals floating at the solution surface. This process of transfer of structural information from 2-D to 3-D systems has proven to be a sensitive tool for understanding the nucleation of various 3-D crystals. For example, optically pure α-amino acid amphiphiles are efficient nucleators for oriented crystals of glycine[1,2] and sodium chloride.[3] Long chain phosphonate[4] and sulfate monolayers[5] were shown to influence the morphology and orientation of barium sulfate crystals nucleated from the subphase. Oriented nucleation of vaterite, the less stable polymorph of calcium carbonate, can be induced by stearic acid monolayers.[6,7] Long chain fatty acids were found to induce the epitaxial formation of PbS crystals[8] and of differently oriented crystals of sodium chloride,[9] and alcohol amphiphiles were found to be efficient ice nucleators.[10] The behavior of all these systems provides evidence for a direct correlation between the structure of the monolayers as 2-D crystalline "nuclei" and that of the mature crystals to be formed. Our long-range study is directed toward a determination of the structural and size requirements for the formation of the ordered aggregates which serve as "nuclei" *en route* to 3-D crystallization.

Here we describe how mixed monolayer films of amphiphilic molecules have been used as models to simulate structured aggregates formed at the air/solution interface and to behave as efficient nucleators of 3-D crystals. The mixed monolayer films are of type **A** + **B**, where the pure amphiphile **A** is an efficient nucleator whereas pure **B** amphiphile is not. The oriented growth of 3-D crystals was studied as a function of the molar ratio of the two components in order to establish the threshold concentration required for efficient nucleation of the crystals. In order to glean information on the structure of the mixed monolayer, we employed the techniques of surface X-ray reflectivity (XR) and grazing incidence X-ray diffraction (GID). The X-ray reflectivity measurements[11] provide information on the electron density profile of the monolayer–solution interface. The GID measurements[12] provide information on the crystal structure of the monolayer.

Results

Design of the 2-D Langmuir Film. Our approach for the design of ordered mixed monolayers with segregated domains of type **A** and **B** took advantage of the packing properties of amide molecules in 3-D crystals,[13] whose molecular arrangements are determined by the hydrogen bonding between the amide groups. By extrapolation, we may expect that hydrogen bonding between amide groups in 2-D films can be a driving force for the formation of a mixed monolayer with the desired characteristics. The component molecules **A** and **B** should fulfill the following requirements: (a) The amphiphile **A** contains a head group appropriate for the induced 3-D crystallization, separated from the amide group by a spacer of appropriate length, (b) The amphiphile **B** contains only the amide head group so as to form intermolecular hydrogen bonds with adjacent molecules of the same or different type, to yield a homogeneous and stable array of hydrocarbon chains, and (c) Within such a mixed monolayer, the interactions involving neighboring amphiphiles **A** favor their segregation into domains.

As amphiphile **A** we used *N*-eicosanoyl-3-aminopropionic acid $CH_3-(CH_2)_{18}-CO-NH-CH_2-CH_2-COOH$ and as inert molecule **B** eicosanamide **1** $CH_3-(CH_2)_{18}-CONH_2$ or behenamide **2** $CH_3-(CH_2)_{20}-CONH_2$. We had chosen the carboxyl moiety as the head group of amphiphile **A** because we could conveniently crystallize metal salts of carboxylic acids as induced by this amphiphile. The proposed molecular arrangement in the mixed monolayers is depicted schematically in Figure 1. We made use of the three methods mentioned above to furnish information on the presence of segregated domains of **A** and **B** within a large uniform net of hydrocarbon chains connected by the hydrogen bonds between their amide groups. There is a central question as to the approximate sizes of such segregated domains as a function of the relative molar ratio of **A**:**B** in connection with the induced nucleation of 3-D crystals. Such knowledge would provide information on the size of the critical nucleus *en route* to 3-D crystallization.

Selection of the Crystal To Be Nucleated by the 2-D Langmuir Film. Spreading of fatty acid amphiphiles on the surface of a solution containing soluble metal carboxylate salts induces an increase in surface concentration of the metal ions bound to the monolayer.[14] Consequently, this surface layer may induce nucleation of metal carboxylate 3-D crystals attached to the

---

[†] The Weizmann Institute of Science.
[‡] Risø National Laboratory.
[●] Abstract published in *Advance ACS Abstracts,* November 1, 1993.

0022-3654/93/2097-12848$04.00/0 © 1993 American Chemical Society

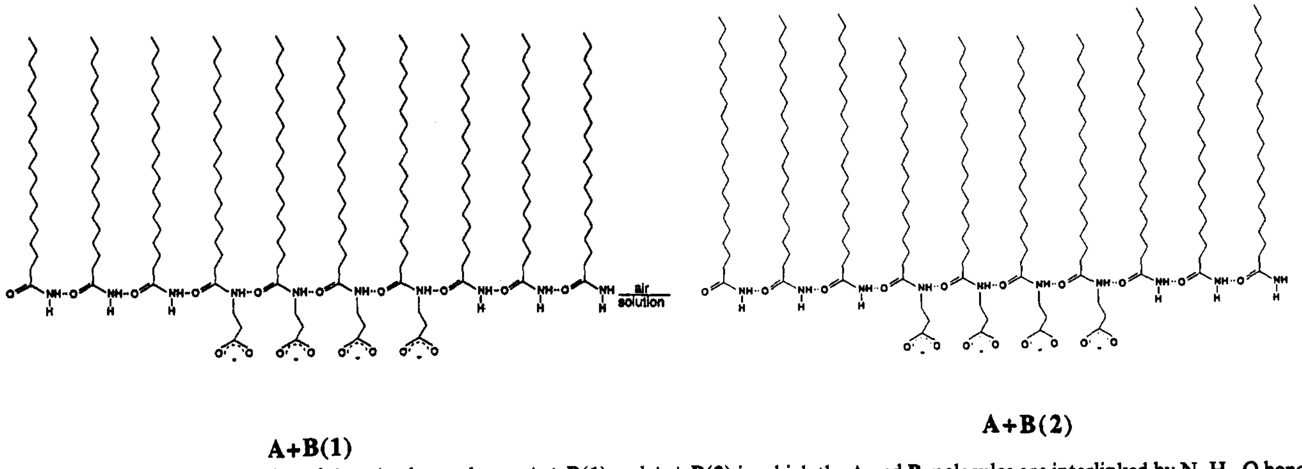

Figure 1. Schematic representation of the mixed monolayers A + B(1) and A + B(2) in which the A and B molecules are interlinked by N–H···O bonds and the A-type molecules form a cluster embedded within the B-type domains.

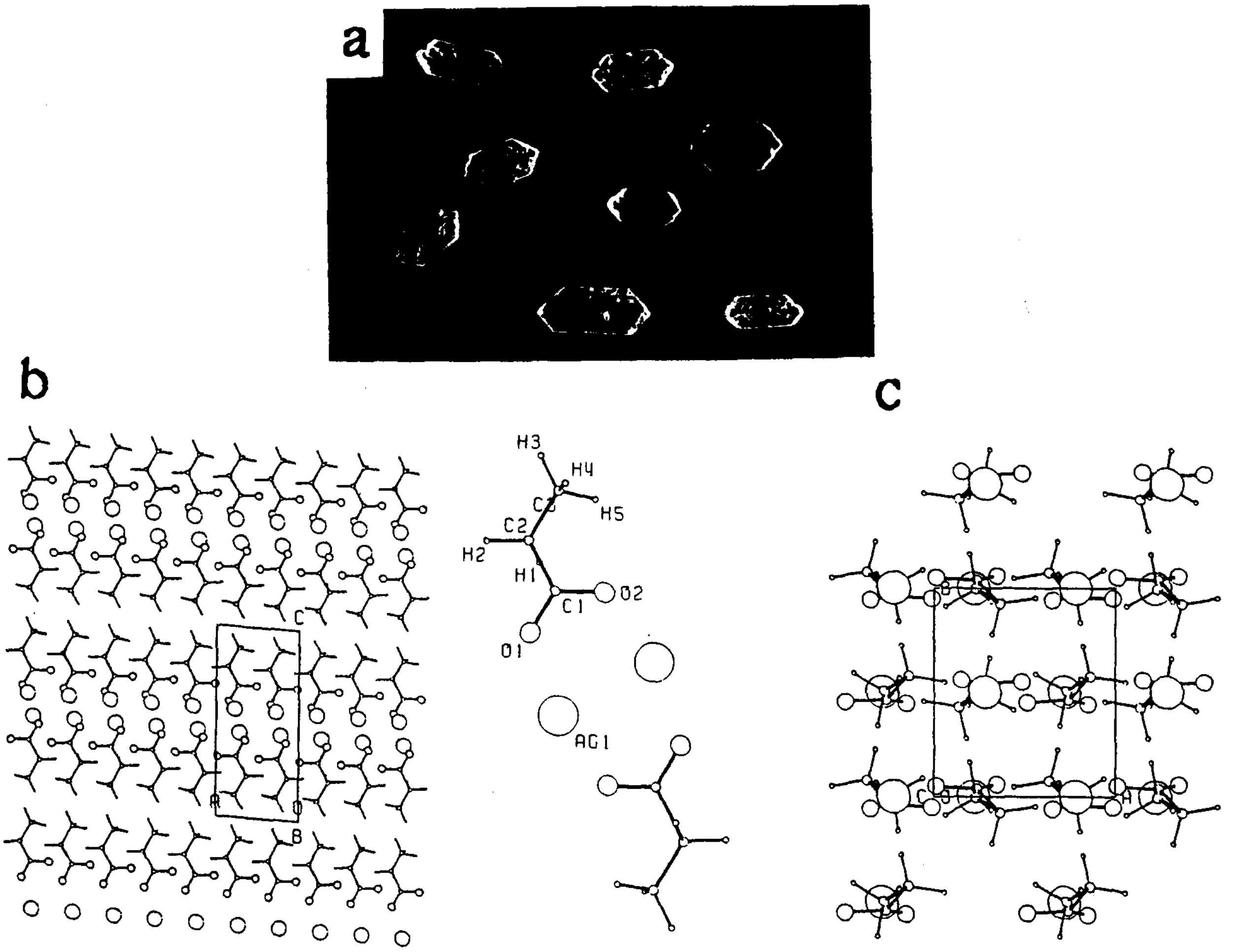

Figure 2. Silver propionate crystal: (a) plate-like {001} morphology of the crystals grown at the air–solution interface, (b) layer-like packing arrangement (and an isolated cyclic dimer) viewed along the *b* axis, and (c) packing arrangement, viewed along the *c* axis, showing the hexagonal distribution of silver ions and molecules within the layer.

interface. The structural requirement for such crystals to be nucleated by the monolayer is that the crystal be composed of bilayers with the metal ions concentrated in planes at the center of each bilayer.

As an appropriate compound, we chose silver propionate CH_3–CH_2–COOAg. Good quality {001} plate-like crystals were obtained by the ionic reaction of equimolar amounts of sodium propionate and silver nitrate in aqueous solutions in the dark. The crystal structure was determined from the X-ray diffraction data collected on an automatic four-circle diffractometer.

Silver propionate crystallizes in the monoclinic space group $P2_1/a$ (a = 5.514 Å, b = 6.302 Å, c = 12.75 Å, β = 86.25°, Z = 4) and contains an *ab* bilayer structure. The bilayer is composed of centrosymmetric cyclic dimers of salt molecules. Within the *ab* bilayer, the dimers are related by translation along *b* and by glide along the *a* axis. Neighboring bilayers make CH_3···CH_3 contacts by translation along the *c* axis to complete the crystal structure. The silver ions are arranged in two closely spaced planes about the center of the bilayer (Figure 2). Crystallization from aqueous solutions (c = 51.6 mM) gave plate-like crystals lying on the bottom of the crystallization dish (crystal density = 2.72 g/cm^3). However, spreading insoluble fatty acid amphiphiles on top of the saturated solution, followed by slow cooling, induced fast crystallization of silver propionate plates floating on the

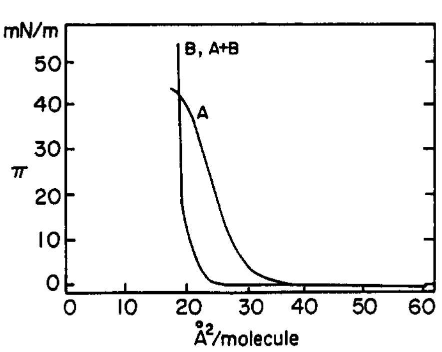

Figure 3. Pressure–area (Π/*A*) isotherm of the monolayer **A** over water and of **B** and **A** + **B** over both water and the ionic solution.

solution surface (Figure 2a). This nucleation effect can be explained by silver ions binding to the monolayer spread over the ionic solution and the formation of local high ion concentration which induces the crystallization. Since surface-induced nucleation of silver propionate crystals depends on the Ag^+ ion binding to the monolayer COO^- groups only, the designed bifunctional amphiphile **A** is also an efficient crystal nucleator.

Crystallization experiments under monolayers of fatty alcohols or esters did not result in floating crystals of silver propionate. Amide monolayers of amphiphiles **B(1)** or **B(2)** caused the appearance of a very small number of floating crystals of a completely different morphology, which were not attached to the monolayer through a well-developed (001) face.

Surface Crystallization Induced by Mixed Monolayers. Surface pressure–area (Π/*A*) isotherms of the pure compounds **A** and **B(1)** or **B(2)** gave a limiting area/molecule of 22.5 and 19.5 Å², respectively. Monolayer mixtures **A** + **B(1)** or **A** + **B(2)**, in the **A**:**B** molar ratio ranging between 1:1 and 1:10, gave a limiting area/molecule similar to that of pure compound **B(1)** or **B(2)** (Figure 3). This result is consistent with the idea that in the mixture, compound **A** tends to adopt the structure of **B**, which serves as a matrix. Spreading such mixtures over the solution containing the appropriate ions followed by compression at 20 °C and slow cooling to 15 °C induced crystallization, after 4–6 hours, of many well-developed {001} plates of silver propionate crystals attached to the monolayer film. From the same solution, but uncovered by monolayer, crystallization occurred only at the bottom of the vessel and at a much slower rate. Oriented crystallization of {001} plates of silver propionate occurred even at low concentration of **A**, down to a 1:10 molar ratio of **A**:**B**. Crystallization in the presence of a mixed monolayer with a molar ratio of **A**:**B** of 1:20 induced the formation of a relatively small number of floating crystals of morphology similar to those obtained using the pure type **B** amphiphile.

The efficient nucleation of oriented silver propionate crystals is consistent with the formation of segregated domains of amphiphile **A** embedded within the inert matrix of the **B** component (Figure 1), even at very low concentrations of the amphiphile **A**. Experiments were performed in order to prove that a *random* monolayer mixture of two amphiphiles **A′** + **B′** would not induce surface crystallization of silver propionate. For this purpose we used stearic acid as **A′** and stearoyl alcohol or methyl stearate as **B′**. Mixtures of **A′** and **B′** in molar ratios of 1:10 to 1:1 did not induce the formation of silver propionate crystals attached at the solution–monolayer interface. Based on the 2-D crystal structures of long chain fatty acids and alcohols,[15] in the relaxed state over pure water, as determined by GID, there appears to be no pronounced driving force for their separation in a binary mixture; indeed the cross-sectional area of the two different head groups complement one another so as to allow effective packing of the aliphatic chains.

Specular X-ray Reflectivity Measurements. X-ray specular reflectivity, as a surface sensitive technique, provides information on the 2-D film thickness, density, roughness, and ion binding.[16]

TABLE I: Fitted Parameters[a] for the Mixed Monolayers Spread on a 1 mM $CdCl_2$ Aqueous Solution in a Three-Box Model

monolayer	coverage	A_m	N_1[b]	L_1	N_2	L_2	N_3	L_3	σ
A + **B(1)** 1:1	0.90	20.5	43	3.5	45	4.7	153	22.0	2.7
A + **B(1)** 1:2.65	0.90	20.5	33	3.7	48	5.1	153	22.5	2.9
A + **B(2)** 1:1	0.90	20.5	43	3.2	39	4.6	161	23.4	**5.2**
A + **B(2)** 1:1.8	0.90	20.5	35	3.2	45	4.8	163	23.7	2.6

[a] A_m is in Å², N in electron unit, L in Å, and σ in Å. [b] The number of electrons in each box was calculated as an average according to the molar fraction of the components; molecules of water were added when **B** component is missing.

TABLE II: Fitted Parameters for the B-type Amphiphiles Spread on a 1 mM $CdCl_2$ Aqueous Solution in a Two-Box Model

monolayer	coverage	A_m	N_1	L_1	N_2	L_2	σ
B(1) pure	1.0	19.5	23	2.6	156	23.0	2.5
B(2) pure	1.0	19.0	23	2.7	169	25.9	2.3

The structural information derived from the specular reflectivity curve can be correlated to certain regions thereof which are sensitive to a given parameter. Thus, the overall thickness of the layer is given by the location of the first intensity minimum corresponding to the first destructive interference of the reflected X-rays. The contrast at this minimum is determined primarily by the density of the polar head groups. The part of the curve at grazing angles below the first intensity minimum is related to the density of the chains. The intensity maximum at higher angles is sensitive to the increased density of the head group of the monolayer due to the binding of ions or specific solute molecules from the subphase. The monolayer roughness results in a continuous decrease in intensity but the effect becomes more pronounced at higher scattering angles. This roughness may arise from the static and thermal diffuseness of the interface.

We have performed X-ray reflectivity measurements for various monolayer mixtures **A** + **B(1)** and **A** + **B(2)** spread on either water or a 1 mM aqueous solution of $CdCl_2$ at pH = 8.4. The Cd^{2+} ions were chosen for study because they must bind to the COO^- groups of neighboring **A** molecules and they are strong X-ray scatterers.

On the assumption that the driving force for the formation of a stable mixed monolayer comes from the hydrogen bonding between the amide groups, we expected differences in the reflectivity curves arising from a difference in chain length above the amide group (see Figure 1). Consequently, the mixed monolayer **A** + **B(1)** composed of molecules of different total length but having the same chain length above the amide group was expected to form a smooth film at the chain–air interface. The mixed monolayer **A** + **B(2)**, whose components are closer to each other in total length but have different chain lengths above the amide group, was expected to form a rough chain–air interface.

The reflectivity curves are presented in Figure 4 for mixtures **A** + **B(1)** of molar ratios 0:1, 1:1, and 1:2.65 and in Figure 5 for mixtures **A** + **B(2)** of molar ratios 0:1, 1:1, and 1:1.8, spread on 1 mM $CdCl_2$ solution at pH 8.4.

One can see that the reflectivity curves for the two pure amphiphiles **B(1)** and **B(2)** are similar (Figure 4a versus Figure 5a), consistent with no ion binding. Furthermore, from the fitted parameters of the reflectivity curves the length of the chain of the **B(2)** molecule is about 3 Å longer than that of **B(1)**, as expected (see Table II). Results of an analysis of the reflectivity curves for the mixed monolayers are consistent with a stoichiometric binding of the Cd^{2+} ions to the COO^- groups of **A**-type component (Cd^{2+}:COO^- = 1:2). However, the obvious difference in the reflectivity curves of 1:1 **A** + **B(1)** and **A** + **B(2)** mixtures can be rationalized only in terms of their different roughness at the chain–air interface. The curves can be reasonably fitted assuming

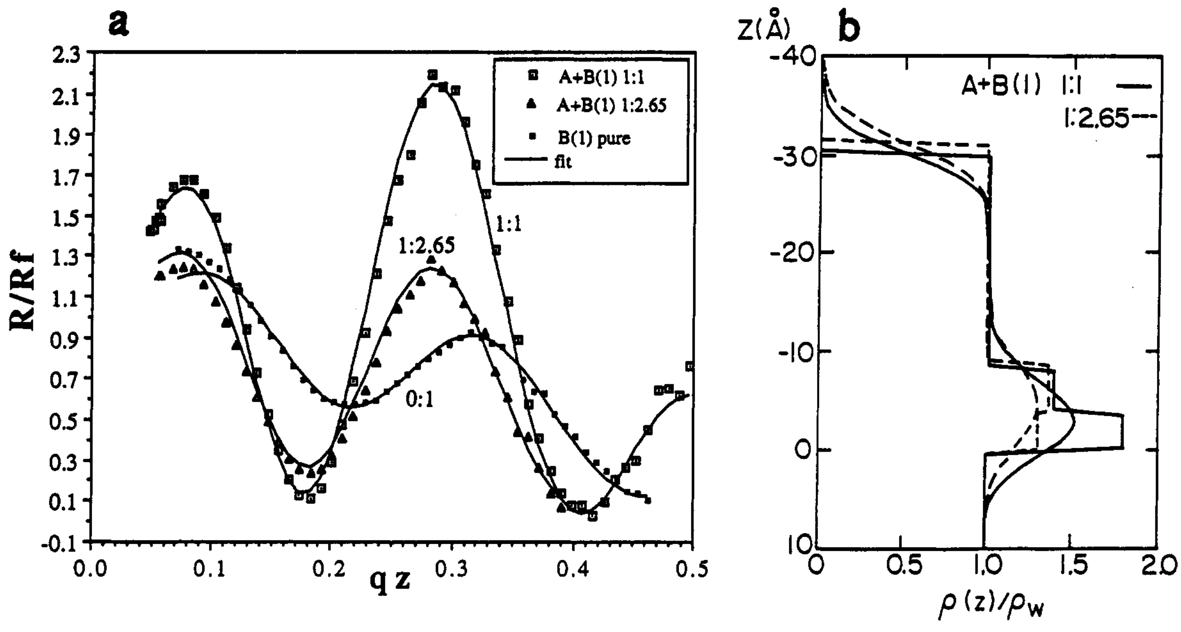

Figure 4. (a) Measured and calculated (full line) reflectivity curves R/R_f for monolayer mixtures A + B(1), of molar ratios 0:1, 1:1, and 1:2.65, over 1 mM $CdCl_2$ aqueous solution at pH 8.4 and temperature 14 °C. (b) Normalized electron density profile of the monolayer $\rho(z)/\rho_w$, where ρ_w is the electron density of the subphase (according to the box model in Table I). The smooth curves represent the electron density profile after the smearing parameter σ has been applied.

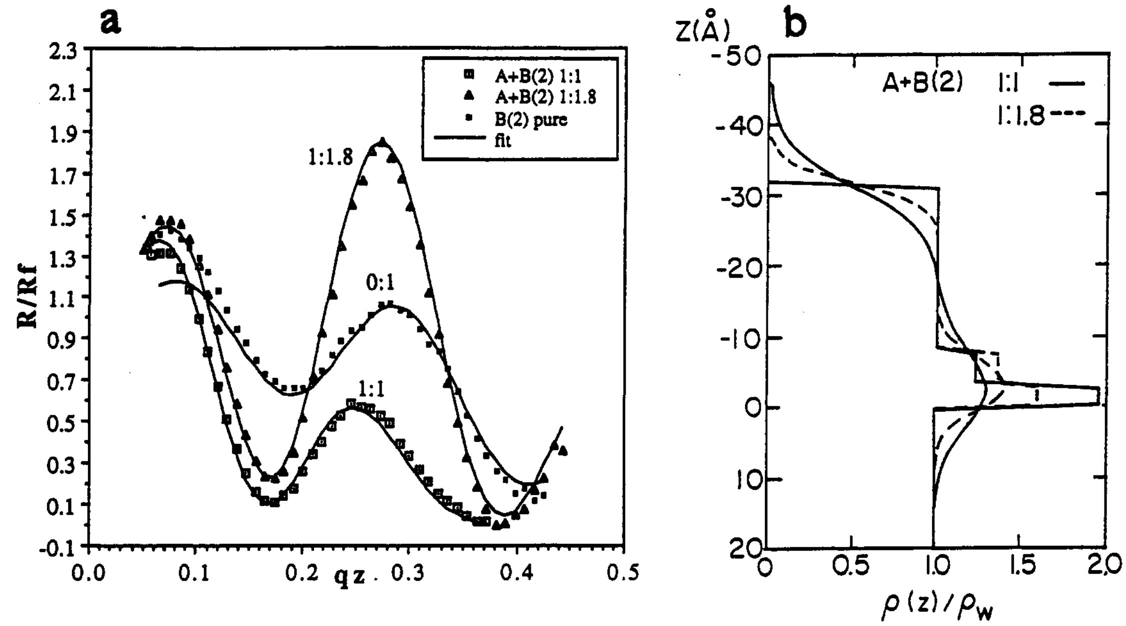

Figure 5. (a) Measured and calculated (full line) reflectivity curves R/R_f for monolayer mixtures A + B(2), of molar ratios 0:1, 1:1, and 1:1.8, over 1 mM $CdCl_2$ aqueous solution at pH 8.4 and temperature 14 °C. (b) Normalized electron density profile of the monolayer $\rho(z)/\rho_w$, where ρ_w is the electron density of the subphase (according to the box model in Table I). The smooth curves represent the electron density profile after the smearing parameter σ has been applied.

for the A + B(2) mixed monolayer a roughness parameter σ = 5.2 Å (see Table I), corresponding to a rough chain–air interface according to the model proposed in Figure 1b. In contrast, the roughness parameter for the 1:1 A + B(1) mixture has a normal value of 2.7 Å. In addition, the fact that the 1:1.8 molar ratio of the A + B(2) mixture has a higher maximum at q_z = 028 Å^{-1} than the 1:1 molar ratio (Figure 4b) is consistent with a smoother film of σ = 2.6 Å when the shorter A component has a lower concentration. One cannot explain the increase in the intensity of the maximum at q_z = 0.28 Å^{-1}, in going from a 1:1 to a 1:1.8 A + B(2) mixture, in terms of the increase in density of the head groups, because fewer COO^- groups are available for cadmium ion binding.

Further evidence for the formation of A-type domains embedded within the B matrix can be obtained from a comparison of the reflectivity curves of the A + B(1) mixed monolayers with molar ratios of 0:1, 1:1, 1:2.65, 1:4.3, and 1:8.1 spread on 1 mM $CdCl_2$ solution (Figure 6). The general trend shows the following features: (i) a rise in the intensity of the maximum at q_z = 0.28 Å^{-1} on increasing the concentration of the A component which binds Cd^{2+} ions, (ii) a shift of the position of the first minimum to lower q_z values consistent with a structure composed of less tilted chains while increasing the concentration of A; such an effect was already reported in other studies where Cd^{2+} ions binding to a fatty acid monolayer forces the molecules to form a less tilted film,[11,17] and (iii) a gradual reduction of the relative intensity of the first minimum with increased concentration of the A amphiphile, as expected from the increased contribution of the Cd^{2+} ion binding.

In another set of experiments, we compared the reflectivity

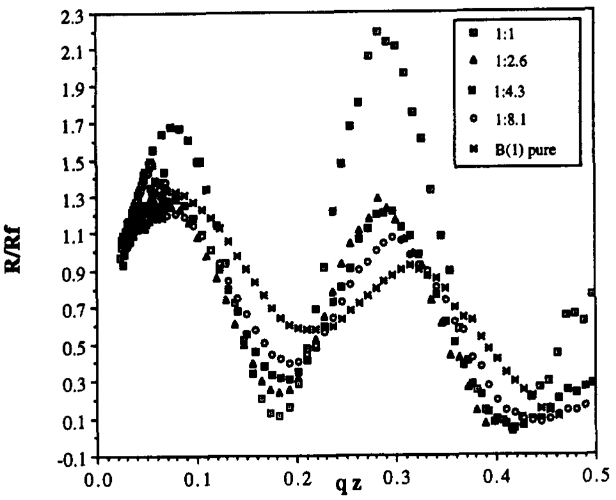

Figure 6. Comparison of the measured reflectivity curves R/R_f for uncompressed monolayer mixtures **A** + **B(1)** spread over 1 mM $CdCl_2$ aqueous solution at pH 8.4 and 14 °C, for various molar ratios of **A** and **B**.

TABLE III: Fitted Parameters for the Mixed Monolayer A + B (1) 1:2.65 Spread on Water and on a 1 mM $CdCl_2$ Solution

subphase	coverage	A_m	N_1	L_1	N_2	L_2	N_3	L_3	σ
0.001 M $CdCl_2$	0.90	20.5	33	3.7	48	5.1	153	22.5	2.9
water	0.93	20.5	31	4.5	48	5.4	153	21.7	2.8

TABLE IV: Fitted Parameters for the Mixed Monolayer A + B (1) 1:4.3 Spread on Water and on a 1 mM $CdCl_2$ Solution

subphase	coverage	A_m	N_1	L_1	N_2	L_2	N_3	L_3	σ
0.001 M $CdCl_2$	0.90	20.5	31	3.5	47	5.0	153	22.0	2.8
water	0.93	20.5	33	4.5	47	5.5	153	21.0	2.8

TABLE V: Fitted Parameters for the Mixed Monolayer A + B(1) 1:8.1 Spread on Water and on a 1 mM $CdCl_2$ Solution

subphase	coverage	A_m	N_1	L_1	N_2	L_2	N_3	L_3	σ
0.001 M $CdCl_2$	0.90	20.5	25	3.5	47	5.2	153	22.5	2.7
water	0.90	20.5	33	4.5	47	5.5	153	21.2	2.6

curves of the **A** + **B(1)** mixtures of various compositions spread on 1 mM $CdCl_2$ solutions and water subphases (Figure 7). It is remarkable that even for the 1:8.1 ratio of the **A** + **B(1)** mixture (Figure 7c), the curves show a visible difference between the reflectivity measured on pure water and that measured on solution which can be attributed to the Cd^{2+} ion binding. In other words, the results suggest that even at such low concentration, domains of **A** are still formed and the ions are bound to adjacent molecules. The following systematic differences can be obtained from the fitted parameters (see Tables III–V). The thickness of the head groups of the mixed monolayers over $CdCl_2$ solution are about 1 Å narrower than that over pure water.[18] Second, the chain length of the mixed monolayer over $CdCl_2$ is about 1 Å longer than that over pure water. These two results are consistent with those obtained for fatty acid monolayers. We therefore propose that the mixed monolayers contain islands of **A** embedded in **B**, which are sufficiently large yet homogeneously distributed that they induced, even at a molar ratio of 1:8.1 **A** + **B(1)**, the **B(1)** molecules to be less tilted. Such a behavior is also in agreement with the oriented crystallization results and the GID.

Grazing Incidence X-ray Diffraction Measurements. Here we present the comparative GID studies performed for the **A** + **B(1)** mixed monolayer of ratio 1:2.92 spread on water and on a 1 mM $CdCl_2$ solution at pH = 8.7. The two diffraction patterns (Figures 8 and 9 and Table VI) are distinctly different, showing the effect of bound ions on the structure of the mixed monolayer.

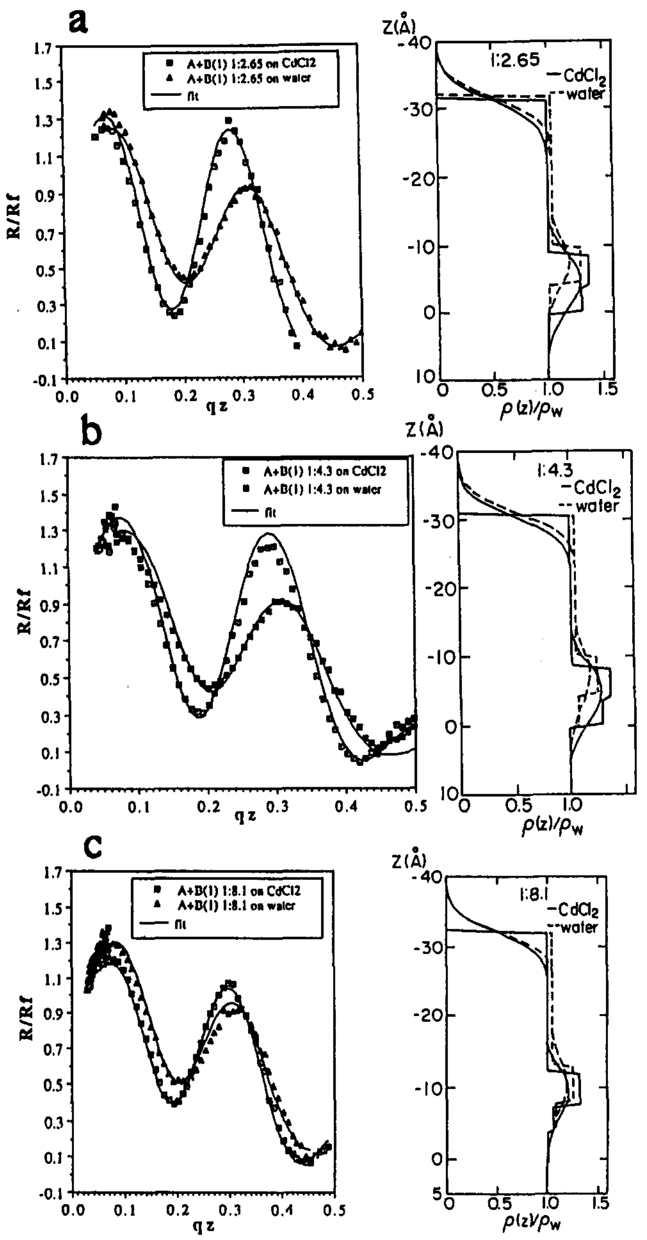

Figure 7. Comparison of the measured and calculated (full line) reflectivity curves R/R_f and normalized electron density profiles $\rho(z)/\rho_w$ for the various monolayer mixtures **A** + **B(1)** spread over 1 mM $CdCl_2$ solution at pH 8.4 with the same monolayer spread over pure water. **A** + **B** molar ratios: (a) 1:2.65, (b) 1:4.3, and (c) 1:8.1.

The mixed monolayer spread on water has the same cell dimensions and chain tilt as reported previously[15] for pure **B(1)**, which is in this case the major component. The two diffraction peaks at q_{xy} = 1.44 Å^{-1} and at 1.52 Å^{-1} (d-spacings of 4.36 and 4.14 Å^{-1}, respectively) were respectively assigned as the {0,2} and the coinciding {1,1} and {1,$\bar{1}$} reflections (Figure 8a) in a rectangular unit cell, the dimensions of which are a = 4.69 Å and b = 8.71 Å. The Bragg rod profile corresponding to the {0,2} reflection (Figure 8b) has its maximum at a q_z value close to the horizon. Hence the molecular axis lies in a plane perpendicular to the b axis. The Bragg rod profile of the {1,1} + {1,$\bar{1}$} peak (Figure 8c) has a maximum at q_z = 0.42 Å^{-1}, indicating that the molecules are tilted at an angle of 18° from the vertical, toward the a axis (Figure 10b).

To confirm the 2-D structure, the Bragg rod intensity profiles were calculated using an atomic coordinate model with 25% occupancy of the **A** molecules. The model was constructed assuming that the molecular chains are related by glide symmetry.[19] The justification therein arises from the presence of a

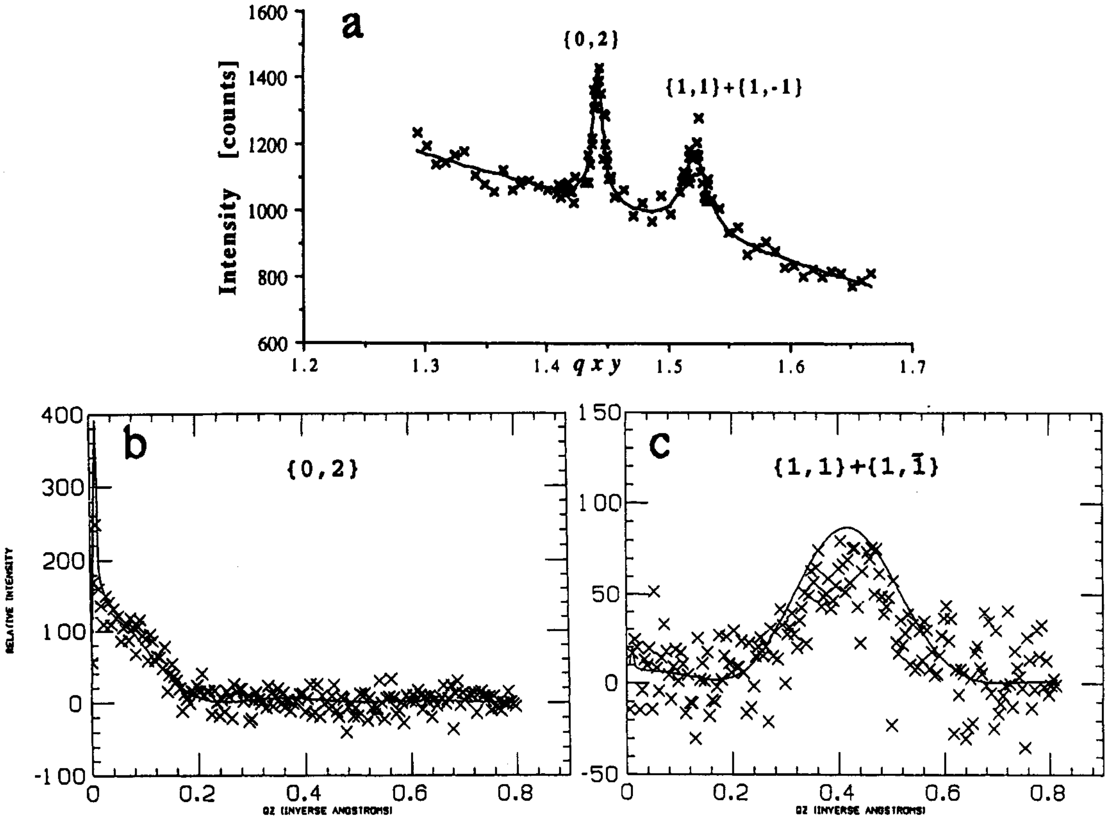

Figure 8. Grazing incidence X-ray diffraction (GID) pattern of the monolayer mixture A + B(1) of molar ratio 1:3 spread over water at $\Pi = 1$ mN/m and 5 °C: (a) Measured and fitted (full line) Bragg peaks of the two reflections $\{0,2\}$ and $\{1,1\} + \{1,\bar{1}\}$. (b and c) Measured and calculated (full line) Bragg rod intensity profiles for the $\{0,2\}$ reflection and the $\{1,1\} + \{1,\bar{1}\}$ reflection.

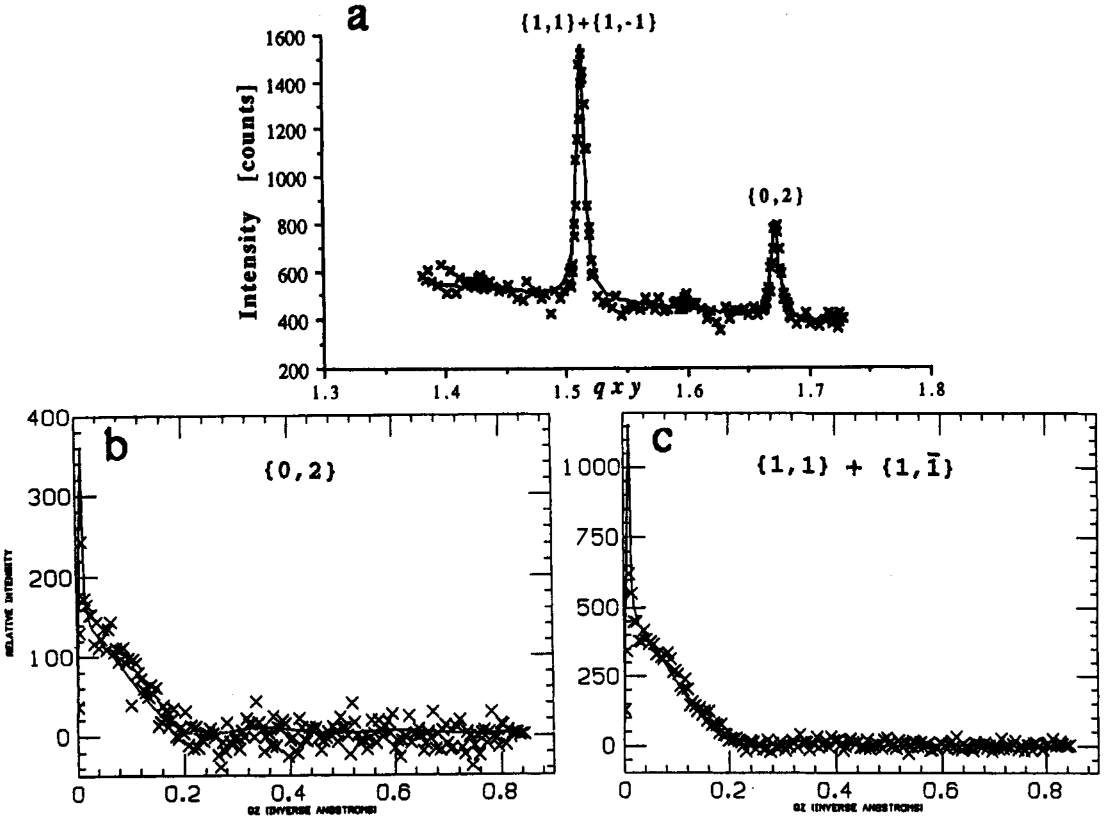

Figure 9. Grazing incidence X-ray diffraction (GID) pattern of the uncompressed ($\Pi = 0$ mN/m) monolayer mixture A + B(1) of molar ratio 1:3 spread over $CdCl_2$ solution pH 8.7 at 5 °C: (a) Measured and calculated (full line) Bragg peaks of the two reflections $\{1,1\} + \{1,\bar{1}\}$ and $\{0,2\}$. (b and c) Corresponding Bragg rod intensity profiles for the $\{0,2\}$ reflection and the $\{1,1\} + \{1,\bar{1}\}$ reflection.

rectangular cell. The chain axes lie halfway between the glide planes in order to ensure good van der Waals interchain contacts. Since the molecular chains are tilted along the *a* direction, the glide plane must be parallel to *a*. The triple requirement for N–H···O(amide) and O–H···O(carboxyl) hydrogen bonding along the *a* axis and van der Waals contacts between chains along *a*

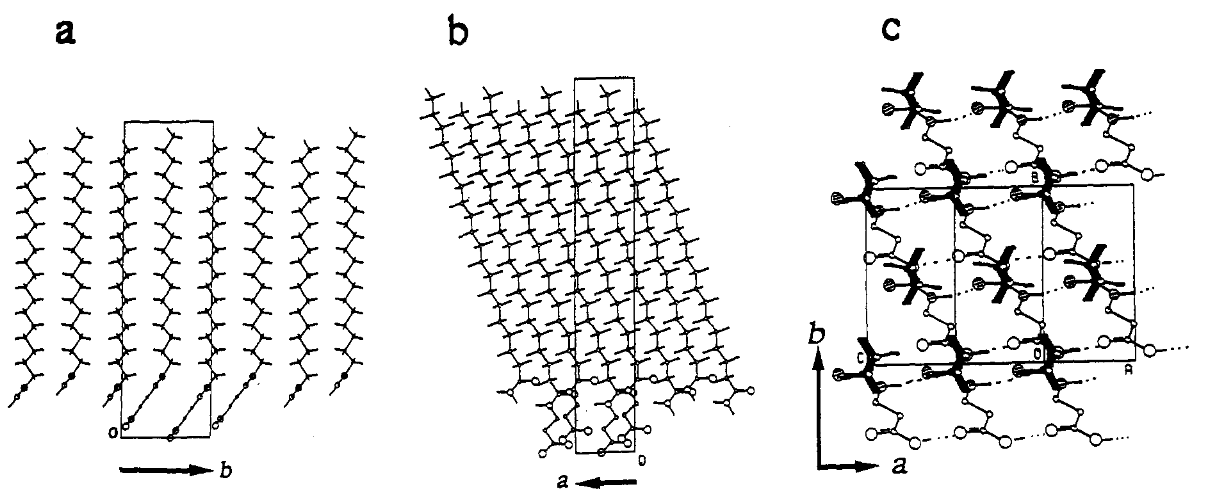

Figure 10. Packing arrangement of the monolayer A + **B**(**1**) of molar ratio 1:3 over pure water at Π = 1 mN/m and 5 °C. Note the essentially glide symmetry along the *a* axis and that the CO–NH–CH$_2$–CH$_2$–COOH moieties are interlinked by N–H···O(amide) and O–H···O(carboxyl) hydrogen bonds. The mixture of **A**- and **B**-type molecules is depicted as viewed along (a) the glide direction *a*, (b) the *b* axis, and (c) the molecular chain axis (the amide oxygen and nitrogen atoms are shaded).

TABLE VI: GID Data of the Mixed Monolayer A + B(1) of Molar Ratio 1:3

	{1,1} + {1,–1}			{0,2}			unit cell	
subphase	q_{xy}	q_z	CL (Å)	q_{xy}	q_z	CL (Å)	*a* (Å)	*b* (Å)
pure water	1.52	0.42	250	1.44	0	800	4.69	8.71
$I_{\{0,2\}/\{1,1\}} = 0.9$								
1 mM CdCl$_2$ solution	1.51	0	>1000	1.67	0	>1000	4.97	7.51
$I_{\{0,2\}/\{1,1\}} = 0.4$								

and *b* demands a dihedral angle of 80° between the planes through –CO–NH–CH$_2$–CH$_2$–COOH and the hydrocarbon chain moieties. In order to prevent interpenetration between the neighboring –CO–NH–CH$_2$–CH$_2$–COOH moieties along the *b* direction, the unit cell was assumed to contain two "independent" molecules. This model was constructed such that the –CO–NH–CH$_2$–CH$_2$–COOH moieties are related essentially by translation along the diagonal $(a + b)/2$ whereas the hydrocarbon chains remain related essentially by the *a* glide symmetry.[20] This arrangement is shown in Figure 10. Note that the two independent molecules are offset by 1.25 Å along the *c* direction. The calculated Bragg rod intensity profiles based on this model are shown in Figure 8, parts b and c.

The mixed monolayer spread on the 1 mM CdCl$_2$ solution at pH = 8.7 has a structure consistent with chains aligned vertically. The GID data (Figure 9a) show a rectangular cell for which the symmetry related {1,1} and 1,$\bar{1}$} reflections coincide at q_{xy} = 1.51 Å^{-1} and the {0,2} reflection is positioned at q_{xy} = 1.67 Å^{-1}. From the Bragg rod profiles (Figure 9, parts b and c) we deduce that the molecules are aligned with their hydrocarbon chains normal to the solution surface. The dimensions of the unit cell (*a* = 4.97 Å, *b* = 7.51 Å) are indicative of the orthogonal (O⊥) packing motif of hydrocarbon chains in which nearest neighboring molecules are related by glide symmetry in a herringbone contact. The length of the *a* axis, 4.97 Å, is fingerprint evidence that the amide groups are hydrogen bonded along this translation axis (Figure 11c). To ensure formation of the N—H·····O=C hydrogen bond, the CO–NH–CH$_2$–CH$_2$–COO$^-$ moiety of the A-type molecules and the –CO–NH$_2$ group of the **B**-type molecules must be rotated by 55° about the first C–C bond above the amide group, out of the plane of the hydrocarbon chain. Furthermore, to achieve reasonable packing of the –CO–NH–CH$_2$–CH$_2$–COO$^-$ and –CO–NH$_2$ groups, the glide plane must be parallel to the *b* axis, resulting in plane symmetry *p*1*g*1 (Figure 11).

The calculated Bragg rods, based on a homogeneous array of chains and amide moieties and only 25% occupancy for the –CH$_2$–CH$_2$–COO$^-$ + 0.5Cd^{2+} groups, fit well the measured intensity profiles (Figure 9 parts b and c).

We interpret this structure in terms of an arrangement composed of clusters of A-type molecules enbedded in a sea of **B** molecules. These A-type clusters would be ideal for Cd^{2+} binding, because each cadmium ion can easily bind to four oxygen atoms of four neighboring COO$^-$ groups interrelated by translation along the *a* axis and by glide symmetry along the *b* axis.

Discussion

The main aim of this work was to prepare a mixed monolayer of amphiphilic molecules A and **B** forming a solid solution, but where A, the active component which induces crystallization of silver propionate, forms domains embedded within the overall cluster. The formation of a stable solid solution is favored by the hydrogen bonds between the amide groups of A and **B**, and the driving force for aggregation of the A molecules is provided by the carboxylate moiety below the amide group. Furthermore, by varying the molar ratio of A:**B** we hoped to obtain a controlled variation of the average size of the A-type clusters to induce nucleation of silver propionate from isolated surface domains.

The crystallization experiments of silver propionate as induced by the mixed monolayers indicated the presence of A-type domains for molar concentrations of A as low as 9%. Mixtures of fatty acids and alcohols and of fatty acids and esters did not yield oriented floating crystals of silver propionate because the two components are randomly arranged within the mixed monolayer. This result is also compatible with the fact that mixed monolayers of fatty alcohols with the length of their chains different by up to four methylene groups were found to be inefficient nucleators of ice as compared to the pure components.[21] GID measurements of such mixed monolayers were consistent with a randomly distributed solid solution.[22]

We made use of Cd^{2+} binding to provide independent evidence in favor of the formation of embedded A-type domains through the specular X-ray reflectivity experiments which indicated complete Cd^{2+} ion binding to the COO$^-$ groups for a molar concentration of A as low as 12%. Because the Cd^{2+} ions must bind to two neighboring COO$^-$ groups to maintain charge neutrality, the result is consistent with the presence of A-type domains.

The GID experiments for the A + **B**(**1**) mixtures in a 1:3 molar ratio show different structures when spread over water and over a CdCl$_2$ solution. Binding of Cd^{2+} induces a highly crystalline mixed monolayer with a lateral coherence length greater than 1000 Å, the resolution limit. The molecular chains are aligned

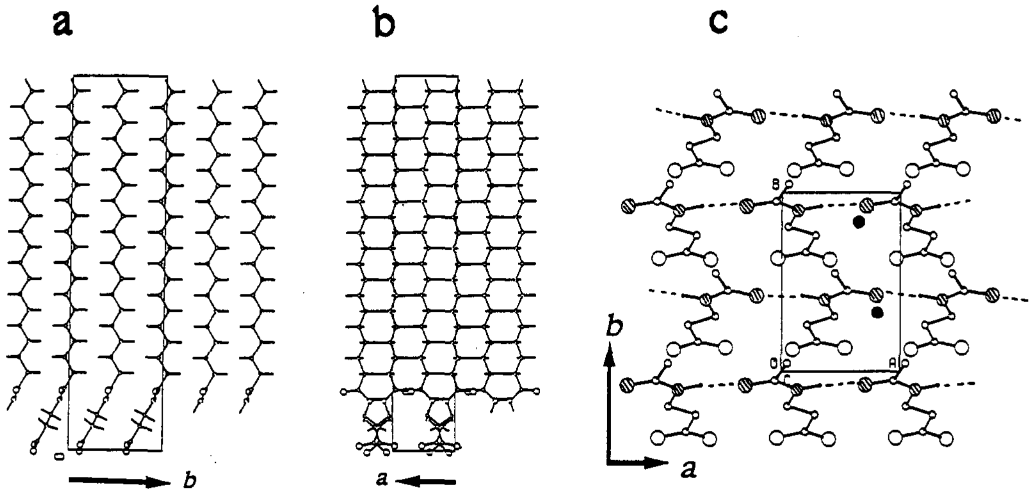

Figure 11. Packing arrangement of uncompressed (Π = 0 mN/m) monolayer **A** + **B**(**1**) of molar ratio 1:3 over $CdCl_2$ solution, pH 8.7, at 5 °C. Note that the vertically aligned hydrocarbon chains are related by glide symmetry along the *b* axis and that the CO–NH moieties are interlinked by N–H···O bonds along the *a* axis. Views along (a) the *a* axis, (b) the *b* axis, and (c) the molecular chain axis. For clarity, the hydrocarbon chains are omitted. Tetracoordinated binding of the Cd^{2+} ions (in full circles) to the oxygen atoms of four neighboring molecules can be achieved as shown (the amide oxygen and nitrogen atoms are shaded).

vertically, with an area per molecule as low as 18.7 Å^2. This structure is different from that on pure water where the major **B** component induces the molecules to adopt a crystalline structure similar to that of the pure **B**, in which the hydrocarbon chains are tilted at an angle of 18° from the vertical and an area per molecule of 20.4 Å^2. According to our model packing arrangement (Figure 11) each Cd^{2+} ion can easily coordinate to four oxygen atoms of four neighboring carboxylate groups and so is conducive for the formation of **A**-type clusters. Because the cadmium: amphiphile stoichiometry is 1:2, each unit cell contains one Cd^{2+} ion. Therefore we propose that the Cd^{2+} ions occupy the two specific sites shown in Figure 11c with an average occupancy of 0.5.

The mixed monolayer **A** + **B**(**1**) of molar ratios 1:1 and 1:2 spread over pure water yielded a packing arrangement[23] similar to that over $CdCl_2$. In this arrangement, the carboxyl groups are also interlinked by O–H···O hydrogen bonds along the *a* axis providing an additonal driving force for **A**-type clustering. Moreover, atom–atom potential energy calculations[24] for **A**- and **B**-type domains show a significant difference of about 18 kcal/mol in the calculated lattice energy, the type **A** domain being more stable.[23]

In the *ab* plane, the unit cell of silver propionate has an area per molecule of 17.3 Å^2 (*ab*/2), which is distinctly lower than the value of 18.7 Å^2 (*ab*/2) obtained from the results for the **A** + **B** mixture in the 1:3 molar ratio over $CdCl_2$ solution. Thus there is no lattice match between the *ab* nets of the monolayer and the (001) face of silver propionate. We therefore interpret the oriented crystallization according to the following sequence: First, formation of centrosymmetric heterodimers between the carboxylate groups of the monolayer and that of the propionate solute molecules, interlinked via a pair of silver ions, akin to the bilayer structure shown in Figure 2. The bilayers generated at the air–solution interface expose toward the solution a two-dimensional array of methyl groups, promoting further bilayer attachment through methyl···methyl contacts. The hydrophobic nature of such contacts across the bilayer surface does not require a precise lattice fit. A lack of a lattice match has already been found in other systems such as in the oriented nucleation of NaCl by α-aminoacid monolayers.[3]

The remaining question to be addressed in this analysis is the *size* of the embedded **A**-type domains, which will provide information as to the size of the nuclei of silver propionate *en route* to crystallization. Such information represents one of the principal unknowns in crystallization processes. We therefore plan to perform small angle grazing incidence X-ray and neutron scattering experiments on **A** + **B**(**1**) mixtures to glean information on the size of the **A**-type domains and where the **A** molecule contains a chain 10 methylene groups longer than the **B**-type molecule, to increase the contrast. We are also planning to use atomic force microscopy to get information on the topography of the mixed monolayer surface.

Experimental Section

Materials. *N*-(Eicosanoyl)-3-aminopropionic acid, **A**, was prepared by the reaction of the sodium salt of the 3-aminopropionic acid with eicosanoyl chloride as the acyl donor, in an acetone/water 1:1 mixture, and by stirring for 4 h. After acidification, the precipitate was isolated by filtration, extracted with hexane, and recrystallized three times from hexane/ethanol 9:1. Purity check: NMR δ (ppm), CH_3 0.88(t), $(CH_2)_{16}$ 1.26(m), CH_2 1.6-(m), $CH_2(COOH)$ 2.33(t), $CH_2(CONH)$ 2.76(t), $CH_2(NH)$ 3.62; IR (cm-1), C=O 1692, C=O(amide) 1635, 1546.

Eicosanamide **B**(**1**) and behenamide **B**(**2**) were prepared from the corresponding acids by reflux with $SOCl_2$ followed by treatment of the dry acyl chloride derivatives with ammonia gas disolved in chloroform. Purity check by IR (cm-1): C=O(amide) 1634, 1547.

Crystallization Experiments. The nucleation of oriented silver propionate (CH_3–CH_2–COOAg) crystals attached under various monolayers was carried out in a teflon Langmuir trough (Feinfabrik, Gottingen, Germany), in the dark. The monolayer solutions (typically 1 mM in chloroform) were spread at 20 °C on the subphase containing a mixture of 200 mL of sodium propionate solution (c = 59.9 mM) with 32 mL of silver nitrate solution (c = 0.374 M). The final concentration is 51.6 mM silver propionate. The monolayer was compressed until about 15 mN/m, and the total area covered by the monolayer molecules, typically 100 cm^2, was kept constant. The crystallization was carried out by slow cooling to 15 °C and occurred after 4–6 h. The surface was covered with many (in the range of hundreds) floating crystals which were collected from the surface after they reached a reasonable size. Crystallization under monolayers which are not efficient nucleators resulted in only very few floating crystals which were collected from the surface. These crystals were very elongated (along the *a* axis) shallow pyramids attached to the surface through their apex "line" and exhibited rough {*h*0*l*} and smooth {0*kl*} faces.

For the solution which was not covered by the monolayer (behind the barrier) crystallization occurred only at the bottom of the trough.

SCHEME I

A+B(1) box model

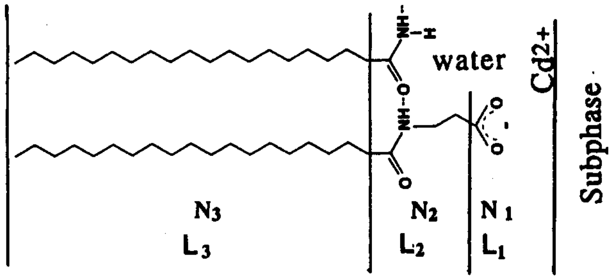

X-ray Structure Determination of Silver Propionate Crystal. The X-ray diffraction data were collected from a silver propionate crystal mounted on a Enraf-Nonius CAD4 diffractometer. The crystal structure was solved by direct methods using the SHELX86 computer program[25] and refined to $R(F) = 0.10$ using the SHELX76 program.[26] The cell constants and atomic coordinates are given in supplementary material.

Set-up for Monolayer X-ray Scattering Experiments. *Specular X-ray reflectivity* (*XR*) experiments were performed on a liquid surface reflectometer constructed at the Risø National Laboratory, Denmark, and mounted on a Rigaku Cu rotating anode generator (operating at 10 kW) in the X-ray laboratory at the Weizmann Institute of Science. The diffractometer is equipped with a sealed and thermostated Langmuir trough which has a Wilhelmy balance for measuring the surface pressure. For the XR measurements, the incident and reflected beam angles are equal and they were varied from $0.5\alpha_c$ to $20\alpha_c$. The detection was made by a NaI scintillation counter mounted behind a graphite monochromator.

XR measurements for various mixtures and pure monolayers were carried out in the uncompressed state ($\Pi = 0$) at a surface coverage of about 90%, both on water and on 1 mM $CdCl_2$ aqueous solution (adjusted to pH = 8.4 with aqueous ammonia), and at 14 °C. Spreading solutions of various mixed or pure monolayers were typically 1 mM in chloroform.

The XR data were analyzed by approximating the electron density $\rho(z)$ profiles perpendicular to the surface with a "box model".[27]

The XR data of the pure **B(1)** and **B(2)** amphiphiles were analyzed in terms of a "two-box model". The first box models the head group ($-CONH_2$) of length L_1 and density ρ_1, whereas the second box represents the hydrocarbon chains of length L_2 and density ρ_2.

The XR data for the various mixed monolayers were analyzed in terms of a "three-box model", on the assumption that the molecules are linked by hydrogen bonds at the level of the amide groups. The first box models the carboxylate group for the mixtures measured over pure water, and carboxylate plus cadmium ions for mixtures measured over $CdCl_2$ solutions (see Scheme I). In each case, the density of the first box was calculated according to the molar fraction of the **A** component, the rest being occupied by water molecules. The second box models the amide group which is common for the two components and the short $-CH_2-CH_2-$ spacer, whose contribution depends on the molar fraction of the **A** component in each mixture. The third box represents the hydrocarbon chains which are of equal length for the **A** + **B(1)** type of mixtures. For the **A** + **B(2)** type of mixtures, the length and the number of electrons in the third box were averaged according to the molar fraction of the **B(2)** component.

The XR data for the **A** + **B(2)** type of mixtures was also analyzed in terms of a "four-box model". Such a model assumes that the third box represents the part of the hydrocarbon chains of equal length for the two components and the fourth box describes the density of the last part of the chains, according to the molar fraction of the longer **B(2)** component. Both types of analysis gave the same fit to the reflectivity curves.

In all the analyses, the parameter A_m represents the limiting area/molecule obtained from the Π/A isotherm upon compression of the film and the monolayer coverage is less than unity since we worked in an uncompressed state.

Grazing incidence X-ray diffraction (*GID*) studies on mixed monolayers were carried out by using the liquid surface X-ray diffractometer[3] on beam line D4 at the synchrotron light source Hasylab, DESY, Hamburg. This diffractometer is also equipped with a sealed and thermostated Langmuir trough and measurements were performed at 5 °C. The trough is provided with a Wilhelmy balance for controlling the surface pressure. For the GID measurements, detection was made by a linear position sensitive detector (PSD) mounted vertically behind the collimating Soller slits of resolution $\delta(2\Theta) = 1.5$ mrad. The GID angle of incidence was $0.85\alpha_c$, where $\alpha_c = 0.138°$ is the critical angle for total external reflection and $\lambda = 1.39$ Å.

The dimensions of the footprint of the incoming X-ray beam on the surface were 50 × 5 mm. The collection of the diffracted beam radiation was made in two ways: the scattered intensity was integrated over the whole q_z window of the PSD yielding Bragg peaks and the intensity was recorded in channels along the PSD but integrated over q_{xy} giving q_z-resolved scans called Bragg rod profiles.

GID measurements were performed for the mixed monolayer spread on a pure water subphase at constant surface pressures $\Pi = 1$ mN/m and $\Pi = 20$ mN/m.[20] The mixed monolayer spread on a 1 mM $CdCl_2$ aqueous solution (adjusted to pH = 8.7 with aqueous ammonia) as a subphase was measured in the uncompressed state ($\Pi = 0$ mN/m) at a surface coverage of about 90%. The spreading solution was a mixed monolayer **A** + **B(1)** 1:2.92 solution in chloroform.

The analysis of the Bragg peaks was as follows: the reflections were indexed by two Miller indices (*hk*), and their $2q_{hk}$ positions were used to calculate the lattice plane spacings $d_{hk} = 2\pi/q_{xy}$, where $q_{xy} = (4\pi/\lambda)\sin q_{hk}$. This data allows for a determination of the unit cell dimensions of the 2-D crystal. The diffraction patterns showed that the monolayer can be considered as a 2-D "powder". Therefore, from the Scherrer formula, $CL \sim 0.9 \times 2\pi/W$, the coherence length CL for each reflection could be evaluated from the resolution-corrected q_{xy} line width *W*.

The variation in intensity $I_{hk}(q_z)$ along a Bragg rod as a function of q_z is proportional to the square of the molecular structure factor amplitude $|F_{hk}(q_z)|^2$. For simple amphiphilic molecules, when the molecules are vertical or tilted in a plane perpendicular to q_{hk}, the maximum intensity along the Bragg rod occurs at the horizon, for $q_z = 0$ Å^{-1}. For molecules tilted otherwise, the Bragg rod maximum occurs at a finite q_z from which the molecular tilt and direction can be evaluated. The structure refinement involving atomic coordinate models was performed as previously described.[24]

Acknowledgment. We thank the Israel Academy of Basic Science and Humanity and the Danish Foundation for Natural Sciences for financial support and Hasylab, DESY, Hamburg, Germany, for beam time.

Supplementary Material Available: Three tables listing the cell constants and atomic coordinates for silver propionate and *N*-eicosanoyl-3-aminopropionic acid in the structure of the 1:3 mixture on water and on Cd^{2+} ions (5 pages). Ordering information is given on any current masthead page.

References and Notes

(1) Weissbuch, I.; Addadi, L.; Leiserowitz, L.; Lahav, M. *J. Am. Chem. Soc.* **1988**, *110*, 561.

(2) Landau, E. M.; Grayer Wolf, S.; Levanon, M.; Leiserowitz, L.; Lahav, M.; Sagiv, J. *J. Am. Chem. Soc.* **1989**, *111*, 1436.

(3) Jacquemain, D.; Grayer Wolf, S.; Leveiller, F.; Lahav, M.; Leiserowitz, L.; Deutsch, M.; Kjaer, K.; Als-Nielsen, J. *J. Am. Chem. Soc.* **1990**, *112*, 7724.

(4) Heywood, B. R.; Mann, S. *Langmuir* **1992**, *8*, 1492.

(5) Heywood, B. R.; Mann, S. *J. Am. Chem. Soc.* **1992**, *114*, 4681.

(6) Mann, S.; Heywood, B. R.; Rajam, S.; Birchall, J. D. *Nature* **1988**, *334*, 692.

(7) Mann, S. *Nature* **1988**, *332*, 119.

(8) Zhao, X. K.; Yang, J.; McCormick, L. D.; Fendler, J. H. *J. Phys. Chem.* **1992**, *96*, 9933.

(9) Landau, E. M.; Popovitz-Biro, R.; Levanon, M.; Leiserowitz, L.; Lahav, M.; *Mol. Cryst. Liq. Cryst.* **1986**, *134*, 323.

(10) Gavish, M.; Popovitz-Biro, R.; Lahav, M.; Leiserowitz, L. *Science* **1990**, *250*, 973.

(11) Kjaer, K.; Als-Nielsen, J.; Helm, C. A.; Tippman-Krayer, P.; Möhwald, H. *J. Phys. Chem.* **1989**, *93*, 3200.

(12) Jacquemain, D.; Grayer Wolf, S.; Leveiller, F.; Deutsch, M.; Kjaer, K.; Als-Nielsen, J.; Lahav, M.; Leiserowitz, L. *Angew. Chem., Int. Ed. Engl.* **1992**, *31*, 130.

(13) Leiserowitz, L.; Hagler, A. T. *Proc. R. Soc. London* **1983**, *A388*, 133.

(14) Zhao, X. K.; Fendler, J. H. *J. Phys. Chem.* **1990**, *94*, 3384.

(15) Jacquemain, D.; Leveiller, F.; Weinbach, S.; Lahav, M.; Leiserowitz, L.; Kjaer, K.; Als-Nielsen, J. *J. Am. Chem. Soc.* **1991**, *113*, 7684–7691.

(16) Daillant, J.; Bosio, L.; Harzallah, B.; Bennatar, J. *J. Phys. II* **1991**, *1*, 149.

(17) Richardson, R. M.; Roser, S. J. *Liq. Cryst.* **1987**, *2*, 797.

(18) Daillant, J.; Bosio, L.; Benattar, J. J.; Blot, C. *Langmuir* **1991**, *7*, 611.

(19) Small, D. M. *The Physical Chemistry of Lipids*; Plenum Press: New York, 1986.

(20) Compression of the mixed monolayer to $\Pi = 20$ mN/m induced a change in the position of the two reflections ($q_{xy} = 1.51$ and 1.66 Å^{-1}) to yield the cell $a = 5$ Å, $b = 7.5$ Å, indicating a motif in which the molecules in the cell are related by glide symmetry. Thus we may safely assume that at low surface pressure, $\Pi = 1$ mN/n, the two molecular chains in the cell are not related by translation, but by a glide along the *a* axis. Although the *a* axis, of length 4.7 Å, is 0.2 Å shorter than the common translation repeat at 4.9 Å for hydrogen-bonded amide systems (see ref 12), the N–H···O distance in our model is 2.9 Å along the *a* axis, which is normal. The O–H···O distance of 2.7 Å along the *a* axis is also satisfactory. In contrast, the monolayer of pure eicosanamide over water in the compressed state does not yield a 5 × 7.5 Å cell, but rather $a = 4.5$ Å, $b = 8.5$ Å. Therefore its packing arrangement in the uncompressed state was determined, on the basis of comparison of the unit cell dimensions with that of 3-D crystals of diamides, to appear in a *c*-centered rectangular cell (see ref 15).

(21) Popovitz-Biro, R.; Majewski, J.; Wang, J. L.; Leiserowitz, L.; Lahav, M. *J. Am. Chem. Soc.* **1993**, accepted for publication.

(22) Wang, J.-L. Manuscript in preparation.

(23) Weissbuch, I.; Leveiller, F.; Jacquemain, D.; Kjaer, K.; Als-Nielsen, J.; Lahav, M.; Leiserowitz, L. *J. Phys. Chem.*, following paper in this issue.

(24) Leveiller, F.; Jacquemain, D.; Leiserowitz, L.; Kjaer, K.; Als-Nielsen, J. *J. Phys. Chem.* **1992**, *96*, 10380.

(25) Sheldrick, G. M., SHELX-86 Computer program for structure determination, Cambridge, England.

(26) Sheldrick, G. M., SHELX-76 Computer program for structure determination, Cambridge, England.

(27) Kjaer, K.; Als-Nielsen, J.; Helm, C. A.; Laxhuber, L. A.; Möhwald, H. *Phys. Rev. Lett.* **1987**, *58*, 2224.